Pharmaceutical Sciences and Drug Design
ISSN: 3062-4428
2026, Volume 6, Issue 1, Page No: 57-71

Available online at: www.galaxypub.co/page/journals

Galaxy Publication

Physicochemical and Bioadhesive Evaluation of Eudragit® EPO/L100 Interpolyelectrolyte Complexes as Gastroretentive Drug Delivery Carriers

Ahmed Mansour[1]*, Omar Saeed[1]

[1]Department of Pharmaceutical Sciences and Drug Development, Faculty of Pharmacy, Cairo University, Cairo, Egypt.

* **E-mail** ✉ ahmed.mansour@gmail.com

Received: 12 October 2025; **Revised:** 05 February 2026; **Accepted:** 07 February 2026

ABSTRACT

This study evaluated interpolyelectrolyte complexes (IPECs) formed from Eudragit® EPO and Eudragit® L100 as potential platforms for gastroretentive drug delivery systems (GRDDS), using metronidazole (MZ) and acyclovir (ACR) as representative model drugs. The prepared Eudragit® EPO/L100 IPECs, obtained under different pH conditions, exhibited variable swelling behavior in simulated fasted gastric fluid (0.1 M HCl) while retaining structural integrity for 6 h. Changes in the internal microenvironment of IPEC matrices under acidic conditions were analyzed by FT-IR spectroscopy, complemented by thermal and elemental characterization. The IPEC formulations exhibited notable bioadhesive performance, with no statistically significant difference from the reference material (Carbopol) in mucin compact adhesion testing. Drug release studies indicated that the liberation of metronidazole (class I BCS) from the IPEC matrices was positively correlated with the extent of swelling. After 6 h in simulated gastric medium (0.1 M HCl), IPEC 1 released 49.62% ± 6.20% of metronidazole, whereas IPEC 2 achieved 87.69% ± 5.15%. In contrast, the cumulative release of acyclovir (class III BCS) reached 25.76% ± 5.67% for IPEC 1 and 21.48% ± 5.00% for IPEC 2. The release behavior of both drugs followed a mechanism governed by polymer chain relaxation within the matrix, consistent with the Peppas–Sahlin kinetic model. Overall, the findings indicate that these interpolymer complexes represent promising candidates for further investigation as carriers in gastroretentive bioadhesive drug delivery applications.

Keywords: Interpolyelectrolyte complexes, Eudragit®, Gastroretentive systems, Drug delivery systems, Bioadhesive systems, Metronidazole

How to Cite This Article: Mansour A, Saeed O. Physicochemical and Bioadhesive Evaluation of Eudragit® EPO/L100 Interpolyelectrolyte Complexes as Gastroretentive Drug Delivery Carriers. Pharm Sci Drug Des. 2026;6(1):57-71. https://doi.org/10.51847/F8c8y5NQl8

Introduction

Gastroretentive drug delivery systems (GRDDS) are designed to enable prolonged retention and targeted drug release in the upper gastrointestinal tract (GIT). These systems are particularly advantageous for drugs with a narrow absorption window in the proximal small intestine [1, 2], as well as for therapies requiring localized action, such as the treatment of inflammatory conditions, cancer, or the eradication of *Helicobacter pylori* infections [3, 4]. To enhance gastric residence time, multiple technological strategies have been developed, including magnetic approaches [5], mucoadhesive formulations [6, 7], expandable systems [8], floating delivery systems [9, 10], high-density dosage forms [11, 12], and polymer-based fibrous constructs [13, 14].

Among these, bioadhesive gastroretentive systems aim to extend drug residence by adhering to the gastric mucosa. Polymers used in such systems typically contain functional groups capable of forming hydrogen bonds, including carboxyl, hydroxyl, amide, and sulfate groups. The adhesion process is complex and involves multiple mechanisms, including electrostatic interactions, adsorption, wetting, diffusion, and mechanical fracture [15, 16]. Frequently utilized bioadhesive polymers include Carbopol®, chitosan, hydroxypropyl methylcellulose (HPMC), and sodium carboxymethyl cellulose (CMC-Na) [17-19]. However, achieving an effective gastroretentive performance often necessitates combining several polymeric excipients within a single formulation.

For example, Naseem *et al*. developed gastroretentive systems incorporating osmotically controlled polymers alongside hydrophilic polymers, hydrophilic gums, gel-forming materials, mucoadhesive components, and microcrystalline cellulose [6]. Zhu *et al*. reported the development of bioadhesive gastroretentive minitablets composed of HPMC, Carbopol® 971P, microcrystalline cellulose, and aerosil [17]. In another study, Ngwuluka *et al*. [20] formulated gastroadhesive matrix systems based on Eudragit® E100, CMC-Na, and locust bean gum, aiming to design a triple-mechanism interpolymeric matrix that integrates high density, swelling capacity, and bioadhesion to achieve controlled zero-order release of levodopa for the treatment of Parkinson's disease.

The application of oppositely charged methacrylate copolymers, including their combinations, to regulate both the site and kinetics of drug release in oral drug delivery systems (DDS) has been extensively reviewed in earlier studies [21, 22]. Furthermore, our research group has previously provided a detailed evaluation of the physicochemical basis governing intermacromolecular interactions in oral DDS formulated using chemically complementary Eudragit® copolymers [23, 24].

In recent years, significant research attention has been directed toward interpolyelectrolyte complexes (IPECs) formed from oppositely charged Eudragit® copolymers [25-37]. This growing interest is largely attributed to the intrinsic structural features of (meth)acrylate copolymers, as Eudragit® polymers possess functional groups with opposing charges, enabling the formation of polycomplexes through intermolecular electrostatic interactions.

At the early stage, the combined effect of two oppositely charged polymers—Eudragit® EPO (EPO) and Eudragit® L100 (L100)—was explored for application in oral controlled drug delivery systems (DDS) [26]. These polymers were incorporated into a polycomplex matrix due to their contrasting hydrophilic and hydrophobic properties, making them suitable for colon-targeted controlled delivery. When these pH-responsive copolymers are blended at an appropriate molar ratio, the resulting EPO/L100 system exhibits controlled diffusion and regulated drug release. FTIR results showed that the samples were unstable under strongly acidic conditions simulating the gastric environment. In contrast, swelling experiments conducted under the same gastric-like conditions showed that all IPEC formulations surprisingly retained their integrity in highly acidic media, despite disruption of ionic interactions.

Considering these findings, further investigations were undertaken to expand this concept by identifying IPEC formulations with potential bioadhesive properties. The objective was to develop sustained gastroretentive drug delivery systems based on polyelectrolyte matrices formed from oppositely charged Eudragit® EPO and Eudragit® L100 [38].

It is recognized that IPEC structures retain ionized functional groups of the original polymers within structural defects, which contribute to their capacity to exhibit bioadhesion when applied in drug delivery systems [39, 40]. In addition, previous studies from our group have shown that EPO demonstrates pronounced mucoadhesive behavior, retaining dye on mucosal surfaces more effectively than free sodium fluorescein. This enhanced retention is most likely due to its cationic character, which facilitates electrostatic attraction to negatively charged mucosal tissues [41].

More recently, we reported that IPECs prepared from Eudragit® EPO/Eudragit® L100-55 copolymers exhibit improved mucosal retention compared to pure EPO. This effect is believed to result from their lower solubility and slower clearance from the mucosal surface [42].

The purpose of the present work was to examine two selected IPEC formulations based on Eudragit® EPO and Eudragit® L100, previously identified as promising GRDDS carriers. This evaluation included assessment of swelling behavior, bioadhesive performance, and drug release characteristics to improve gastric-targeted delivery of two model drugs: metronidazole (MZ) and acyclovir (ACR).

ACR is primarily absorbed in the upper gastrointestinal tract and possesses a relatively short elimination half-life of approximately 2.5 h [43]. Therefore, designing a gastroretentive formulation for ACR could enhance its overall bioavailability.

In contrast, MZ is an antibacterial agent commonly used to treat chronic infections caused by *Helicobacter pylori*, which is strongly associated with the development of peptic ulcers and gastric carcinoma [44]. Developing a formulation that provides localized gastric delivery of MZ may improve therapeutic efficacy and address challenges in current pharmacological treatment strategies.

This study evaluated interpolyelectrolyte complexes (IPECs) formed from Eudragit® EPO and Eudragit® L100 as potential platforms for gastroretentive drug delivery systems (GRDDS), using metronidazole (MZ) and acyclovir (ACR) as representative model drugs.

Materials and Methods

Materials

EPO is a polycationic terpolymer consisting of dimethylaminoethyl methacrylate, methyl methacrylate, and butyl methacrylate in a molar ratio of 2:1:1 (MW 150,000 g/mol). L100 is a polyanionic copolymer composed of methacrylic acid and methyl methacrylate in a molar ratio of 1:1 (MW 135,000 g/mol). Both polymers were used to prepare interpolyelectrolyte complexes (IPECs) and physical mixtures (PhM). These materials were kindly supplied by Evonik Industries AG (Darmstadt, Germany). Metronidazole (MZ) and acyclovir (ACR) were obtained from Merck (Sigma-Aldrich, St. Louis, MO, USA). Mucin derived from porcine stomach (type II) (Merck group, Sigma-Aldrich, St. Louis, MO, USA), along with segments of pig gastric mucosa, was utilized in bioadhesion studies.

Sodium hydroxide (NaOH), reagent grade ≥ 98% (anhydrous pellets) (Sigma-Aldrich, St. Louis, MO, USA), and hydrochloric acid (HCl), 36.5%–38.0% (Sigma-Aldrich, St. Louis, MO, USA), were used to prepare 1 M solutions for pH adjustment. Hydrochloric acid (HCl), 36.5–38.0% (Sigma-Aldrich, St. Louis, MO, USA), was additionally used to prepare a 0.1 M solution simulating the fasted gastric environment.

Preparation of solid interpolyelectrolyte complexes (IPEC) and physical mixtures (PhM)

Solid interpolyelectrolyte complexes based on Eudragit® copolymers were synthesized in aqueous media at pH = 6.0 (IPEC 1) and pH = 6.5 (IPEC 2). Separate solutions of EPO and L100 were first prepared, adjusted to the desired pH values, and subsequently combined following previously reported procedures [26]. The resulting IPEC materials were vacuum-dried using a vacuum oven (VD 23, Binder GmbH, Tuttlingen, Germany), then ground into powder using an automated mixing and grinding device (ShakIR, Pike Technologies, Madison, WI, USA), and finally compressed into matrix forms.

Physical mixtures (PhM) were produced by blending powdered EPO and L100 using the same ShakIR mixing and grinding system (Pike Technologies, Madison, WI, USA).

Preparation of tablets

To obtain matrices for swelling evaluation, IPEC and PhM powders (100 mg, 8 mm diameter) were compressed using a PressPRO 15-ton programmable hydraulic press designed for IR spectroscopy (Pike Technologies, Madison, WI, USA). The compaction was carried out under a pressure of 2.45 MPa.

For drug release experiments, tablets (8 mm diameter) were prepared by combining IPEC or PhM (50 mg) with the respective model drug (100 mg), followed by compression under identical conditions (2.45 MPa) using the same PressPRO 15-ton automated hydraulic press (Pike Technologies, Madison, WI, USA).

Determination of the degree of swelling of matrices

Swelling studies were conducted under simulated fasted gastric conditions using 0.1 M HCl at 37 ± 0.5 °C for 6 h. Each matrix was initially placed into a pre-weighed basket and then immersed in 40 mL of medium within a thermostatically controlled bath (IC control eco 18c, IKA® Werke GmbH, Staufen, Germany). At 30 min intervals, the basket was removed, excess surface liquid was carefully blotted off with filter paper, and the sample was weighed.

The extent of swelling (H%) was determined according to the following expression:

$$H\% = \frac{(m_2 - m_1)}{m_1} \times 100 \quad (1)$$

Where m1 denotes the initial dry mass, and m2 corresponds to the mass measured after swelling.

Elemental analysis

The elemental composition of IPEC samples, both before and after swelling experiments, was determined using a CHNS/O Elemental Analyzer (Thermo Flash 2000, Thermo Fisher Scientific, Paisley, UK). The ratio Z = [EPO]:[L100] (mol/mol) was calculated to express the composition. Before analysis, samples were dried under vacuum at 40 °C for 2 days and weighed using an XP6 Excellence Plus XP microbalance (Mettler Toledo,

Greifensee, Switzerland). The prepared samples were then sealed in crucibles and introduced into the combustion chamber via an autosampler.

The analysis was performed at 900 °C with a gas flow rate of 10 mL/min. Instrument calibration was performed using an atropine standard (Thermo Fisher Scientific, Paisley, UK), and the resulting data were processed using Eager Xperience Data Handling Software (version 1.3.07/2014). Each measurement was repeated three times.

Nitrogen content (%) was used as the determining parameter since nitrogen is present only in EPO. The final composition of IPECs was calculated based on both the molar masses of the original copolymer units and the measured nitrogen percentage in each sample.

Fourier-transformed infrared (ATR-FTIR) spectroscopy

Infrared spectra were acquired using a Nicolet iS5 FTIR spectrometer (Thermo Scientific, Waltham, MA, USA) equipped with a single-bounce ZnSe ATR crystal (iD5). Spectral interpretation was performed using OMNIC software (version 8.2.387).

Thermal analysis

Thermal behavior was examined using modulated differential scanning calorimetry (mDSC) with a Discovery DSC™ instrument (TA Instruments, New Castle, DE, USA) fitted with a refrigerated cooling system (RCS90). Data analysis was conducted using TRIOS™ software (version 3.1.5.3696) (TA Instruments, New Castle, DE, USA).

All measurements were performed in Tzero aluminum pans (TA Instruments, New Castle, DE, USA), while an empty pan served as the reference. The masses of both reference and sample pans were included in calculations. Nitrogen gas was supplied at a constant flow rate of 50 mL/min throughout the experiments. Temperature calibration was performed using indium and n-octadecane standards, enthalpy calibration with indium, and heat capacity calibration using sapphire.

The thermal protocol involved cooling the samples from room temperature to 0 °C, holding them at this temperature for 5 min, and subsequently heating from 0 to 250 °C. A heating rate of 2 °C/min was applied, with a modulation period of 40 s and an amplitude of 1 °C. Glass transition temperatures were determined from the reversal of the heat flow signal. All measurements were carried out in triplicate.

Study of model drug release

Drug release from IPEC- and PhM-based tablets was evaluated for MZ and ACR using a Flow-Through Cell Apparatus integrated with a CE 7 Smart system (Sotax AG, Aesch, Switzerland). The experiments were conducted under conditions simulating the fasted stomach (0.1 M HCl; 37 ± 0.5 °C), using an open-loop configuration at a flow rate of 8 mL/min [37] over 6 h.

Quantification of released MZ and ACR was performed using a UV spectrophotometer Evolution 220 (Thermo Scientific, Waltham, MA, USA) at wavelengths of 274 nm and 202 nm, respectively. Drug concentrations were determined from calibration curves. The resulting release data were analyzed using Microsoft Office 2021 (MSO, Version 2401, Build 16.0.17231.20236) and the zero-order, first-order, and Peppas–Sahlin kinetic models [45, 46].

Analysis of bioadhesive properties

The adhesive performance of IPEC and PhM samples was assessed using a TA.XTplus texture analyzer (Stable Micro Systems, Surrey, UK). Mucin compacts and pig stomach mucosal tissue were employed as model substrates. Mucin compacts were prepared by compressing mucin powder at 2.45 MPa using a 15-ton automated hydraulic press (Pike Technologies, Madison, WI, USA) with a 13 mm die.

Pig stomach tissue was obtained immediately after slaughter from an abattoir and transported on dry ice in a polystyrene container. After thawing, the tissue was sectioned into 3 × 3 cm pieces. Adhesion measurements on mucosal tissue were performed in an acidic medium (0.1 M HCl).

During testing, IPEC or PhM samples were fixed to the probe, while the mucin compacts or tissue samples were positioned on the platform. Carbopol® 2020 (Carbopol) was used as the positive control.

For mucin compacts, the testing parameters were set as follows [20]: pre-test speed 0.5 mm/s, test speed 0.1 mm/sec, post-test speed 0.1 mm/s, applied force 0.1 N, trigger force 0.1 N, and return distance 10 mm. For pig

stomach tissue, the parameters were: pre-test speed 1 mm/s, test speed 0.1 mm/sec, post-test speed 0.1 mm/s, applied force 0.1 N, trigger force 0.1 N, and return distance 10 mm.
Each formulation remained in contact with the substrate for 60 s. Data collection was carried out using Texture Exponent Software (Version 3.2). Gastroadhesive strength was evaluated based on the peak force, defined as the maximum force required to detach the matrix from the mucin compact or tissue surface [20].

Statistical analysis
Each experiment was repeated three times. Statistical processing of the obtained data was performed using Microsoft Office 2021 (MSO, Version 2401, Build 16.0.17231.20236). Results are presented as mean ± standard deviation. Differences between groups were evaluated using one-way analysis of variance (ANOVA) in combination with a t-Test (Two-Sample Assuming Equal Variances). A value of $P < 0.05$ was considered to indicate statistical significance.

Results and Discussion

Composition study
The elemental analysis data **(Table 1)** showed that the composition of the synthesized IPEC systems varied with the pH of the preparation medium. A higher pH led to greater incorporation of the polycation component (EPO) into the resulting polycomplex. Specifically, the sample prepared at pH 6.0 (IPEC 1) showed an almost equimolar ratio (Z = [EPO]/[L100] = 1.02). In contrast, the system synthesized at pH 6.5 (IPEC 2) exhibited a notable excess of EPO, corresponding to a 1.5-fold increase (Z = 1.49). These observations indicate preferential enrichment of the less ionized polymer fraction, particularly evident in IPEC 2.

Table 1. Characteristics of IPEC EPO/L100 systems.

Sample code	Tg (°C)	EPO: L100 (mol/mol)	IPEC composition (Z = [EPO]/[L100])	pH of IPEC formation
IPEC 1	146.6 ± 0.3	1:0.98	1.02	6.0
IPEC 2	117.4 ± 0.2	1:0.67	1.49	6.5

Eudragit copolymers are known to be amorphous and exhibit a characteristic glass transition temperature (Tg) [21, 23]. To examine the structural organization and confirm the homogeneity of the polymer systems, modulated differential scanning calorimetry (mDSC) was used. The absence of multiple Tg values indicated a lack of phase-separated microdomains of individual copolymers. Both IPEC samples displayed a single Tg, with values situated between those of the parent polymers: higher than EPO (52.1 ± 1.3 °C) and lower than L100 (193.3 ± 1.8 °C).

Assessment of the IPEC behavior in acidic medium
To determine their suitability as drug delivery carriers, the stability and behavior of IPEC matrices were examined under simulated fasted gastric conditions (0.1 M HCl). Their performance was directly compared with matrices prepared from physical mixtures (PhMs).
A clear distinction in behavior was observed: PhM-based matrices underwent complete dissolution within 2 h in the acidic medium. In contrast, IPEC matrices did not dissolve but instead expanded, forming hydrogel-like structures that maintained their integrity for the entire 6 h experimental duration **(Figure 1).**
Evaluation of swelling kinetics **(Figure 2)** revealed that IPEC 2 exhibited a more gradual initial swelling during the early stages of exposure. However, over time, this system achieved a significantly higher final swelling degree of 851.53%, compared to 481.54% for IPEC 1.

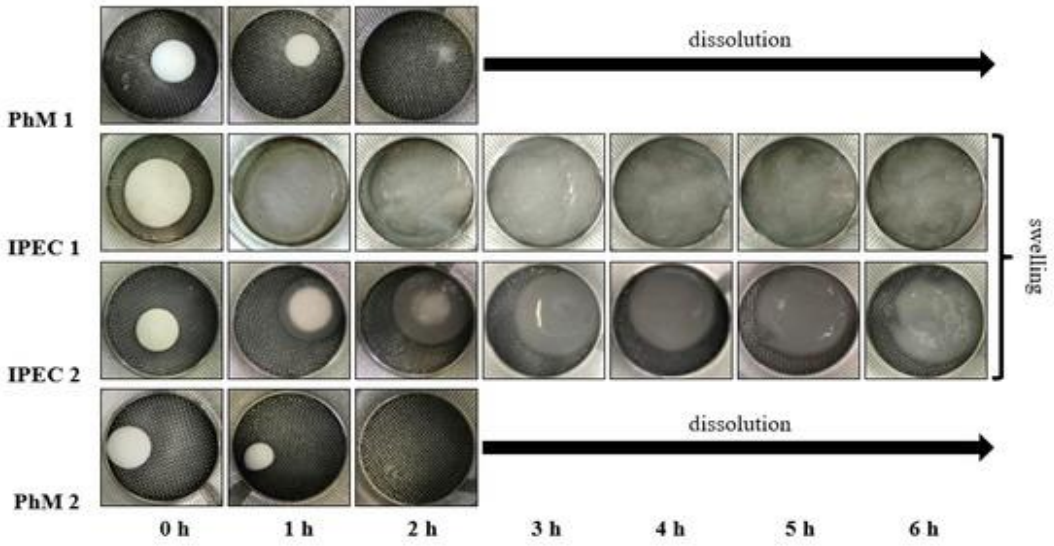

Figure 1. External appearance of IPEC and PhM matrices during the swelling test.

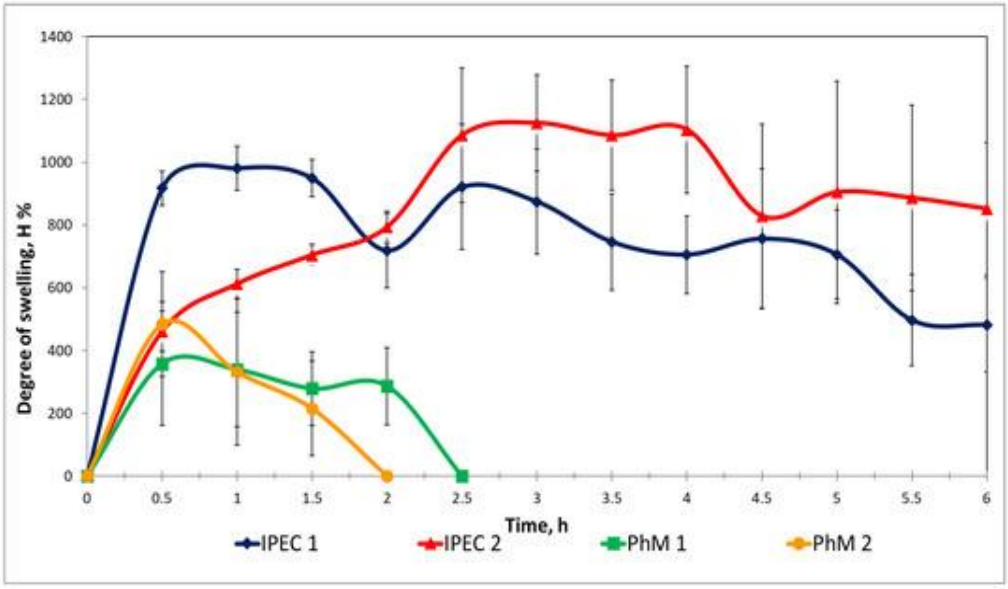

Figure 2. Swelling profiles of IPEC and PhM matrices in mimicking fasted stomach medium (0.1 M HCl) (n = 3, mean ± SD).

The enhanced resistance of IPEC matrices to dissolution can be attributed to their internal structure, which is stabilized by ionic interactions between the protonated dimethylamino groups of EPO and the deprotonated carboxyl groups of L100. The presence of such interactions is confirmed by the emergence of a distinct FTIR band at 1560 cm−1. Analysis of FTIR spectra **(Figures 3 and 4)** showed that the intensity of this band decreased gradually as the residence time in the acidic medium increased, indicating partial disruption of ionic linkages. This structural change is likely responsible for the minor dissolution observed and the corresponding reduction in swelling behavior over time.

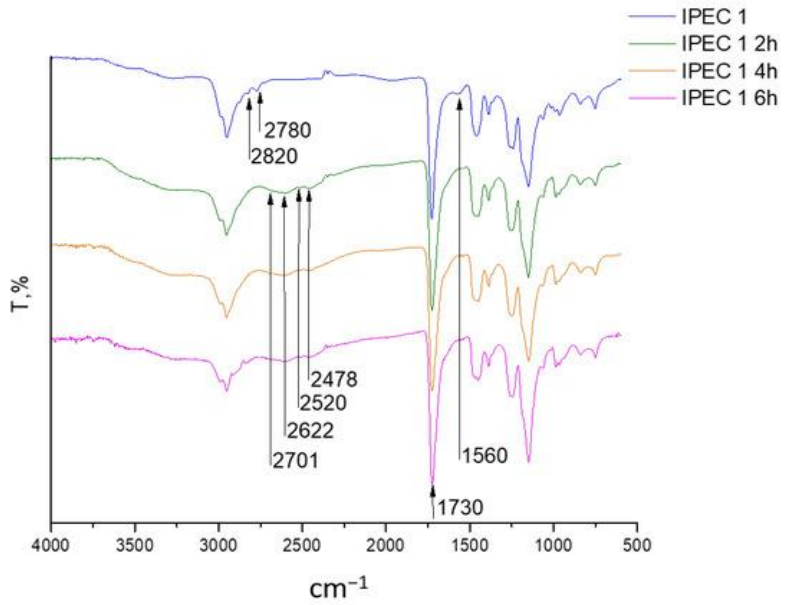

Figure 3. FTIR spectra of IPEC 1 after swelling in mimicking fasted stomach medium (0.1 M HCl).

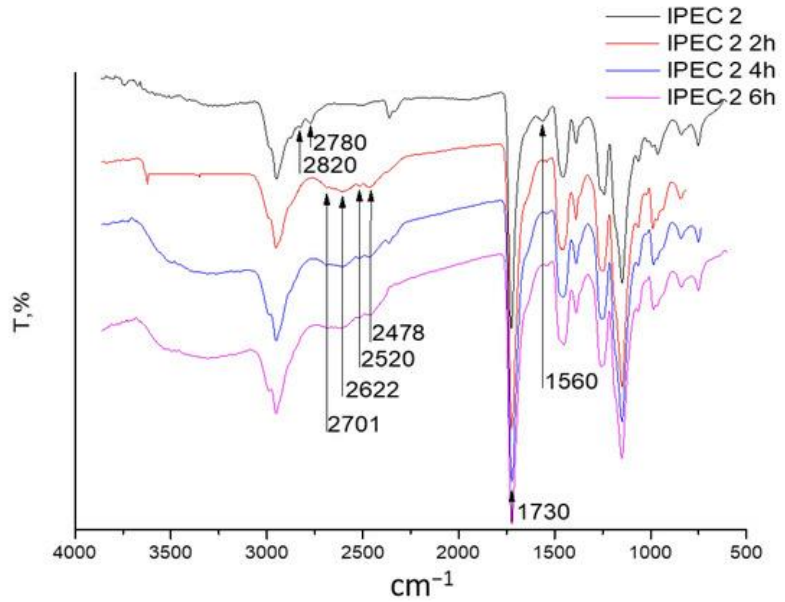

Figure 4. FTIR spectra of IPEC 2 after swelling in mimicking fasted stomach medium (0.1 M HCl).

Further spectral features supported the presence of intermolecular interactions. The broadening of absorption peaks in the region 2520–2478 cm−1 can be attributed to hydrogen bonding between functional groups of the two polymers, specifically involving dimethylamino or carbonyl groups of EPO and hydroxyl groups of L100. Additionally, a wide band observed between 2350 and 2750 cm−1 suggests the formation of various ammonium cation species, including both monomeric and dimeric forms, potentially associated with water molecules. These findings are in agreement with previously reported data [26].

To further elucidate structural evolution during exposure to acidic conditions, mDSC analysis was performed. For IPEC 1, immersion for up to 6 h resulted in a substantial increase in Tg, rising from 117.4 ± 0.2 to 170.6 ± 0.1 °C. Importantly, only a single Tg was observed across all thermograms, confirming that the IPEC systems remained unified structures without separating into individual polymer domains.

Elemental analysis revealed that compositional changes occurred during swelling. As shown in **Table 2**, IPEC 2 (initially Z = 1.49) experienced a significant loss of EPO, resulting in a final composition in which only one-third of the polycation remained relative to L100 (Z = 0.5). A comparable trend was identified for IPEC 1, although the extent of EPO loss was less pronounced.

The observed decrease in EPO content corresponded with changes in Tg values, indicating that leaching of the polycation during exposure to the acidic medium directly influenced the structural properties of the polycomplex. These results are consistent with previously published findings [26].

Table 2. Results of the thermal and elemental analysis for IPEC samples after swelling in mimicking fasted stomach medium (0.1 M HCl) (n = 3, mean ± SD).

Sample code	Nitrogen content (N, %)	IPEC composition (Z = EPO:L100, mol/mol)	Glass transition temperature (Tg, °C)
IPEC 1–2 h	2.84 ± 0.16	1:1.17	165.8 ± 0.1
IPEC 1–4 h	2.91 ± 0.26	1:1.11	170.7 ± 0.1
IPEC 1–6 h	3.11 ± 0.10	1:1.08	170.6 ± 0.1
IPEC 2–2 h	2.78 ± 0.11	1:1.22	169.5 ± 0.1
IPEC 2–4 h	2.54 ± 0.12	1:1.47	172.3 ± 0.5
IPEC 2–6 h	2.75 ± 0.31	1:1.27	173.9 ± 0.3

Despite these compositional and structural transformations, the swelling study demonstrated that the integrity of the IPEC matrices was preserved for 6 h under acidic conditions. These findings suggest that such systems possess sufficient stability to warrant further development as carriers for gastroretentive drug delivery systems (GRDDS).

Analysis of bioadhesive properties

Adhesion typically develops in two sequential phases: an initial contact phase followed by a consolidation phase. In the first phase, the dosage form comes into contact with the mucosal surface, where the polymer begins to hydrate, leading to swelling and softening. The second phase involves the establishment of molecular interactions between polymer chains and mucin, resulting in stable adhesion bonds [20, 47].

Differences in mucoadhesive performance were observed depending on whether mucin compacts or actual gastric tissue were used as substrates. While mucin compacts are useful for screening adhesive potential, they cannot fully reproduce the complexity of biological tissue, as confirmed in this study. The contact between the tablet and the mucin compact is highly uniform, ensuring excellent reproducibility of results. Under these conditions, the adhesion force of Carbopol (positive control) did not differ significantly from that of either the IPEC or the PhM formulations. Peak positive force values measured on mucin compacts are shown in **Figure 5**.

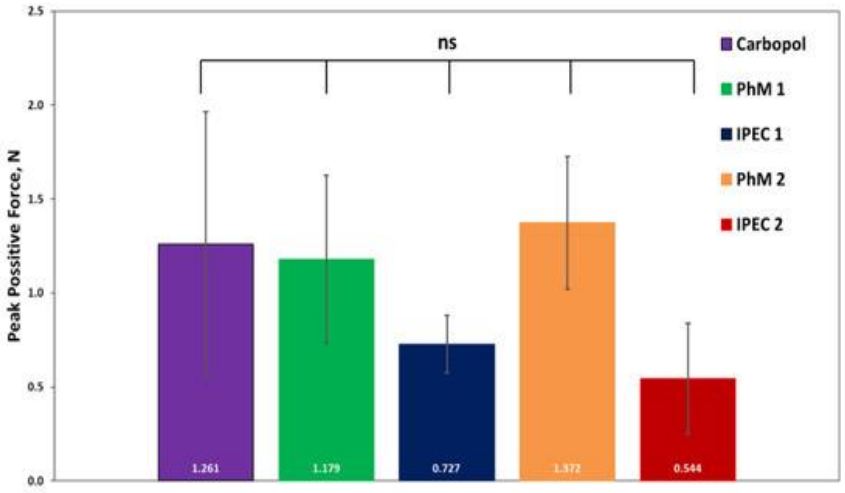

Figure 5. Results of measuring peak positive force of IPECs and PhMs from mucin compacts (N) (n = 3, mean ± SD, "ns" represents not significant).

Overall, both IPECs and PhMs demonstrated mucoadhesive behavior comparable to Carbopol. To obtain more physiologically relevant data, adhesion testing was repeated using pig stomach mucosa. The corresponding peak force values are presented in **Figure 6**.

Adhesion to gastric tissue is influenced by multiple variables, including hydration state, anatomical region of the stomach, and available contact area. In this model, Carbopol showed stronger adhesion than both IPEC and PhM

systems. However, excessively strong adhesion in gastroretentive formulations may be undesirable, as it can result in unintended attachment in the esophagus or throat, potentially causing tissue irritation or damage [47].

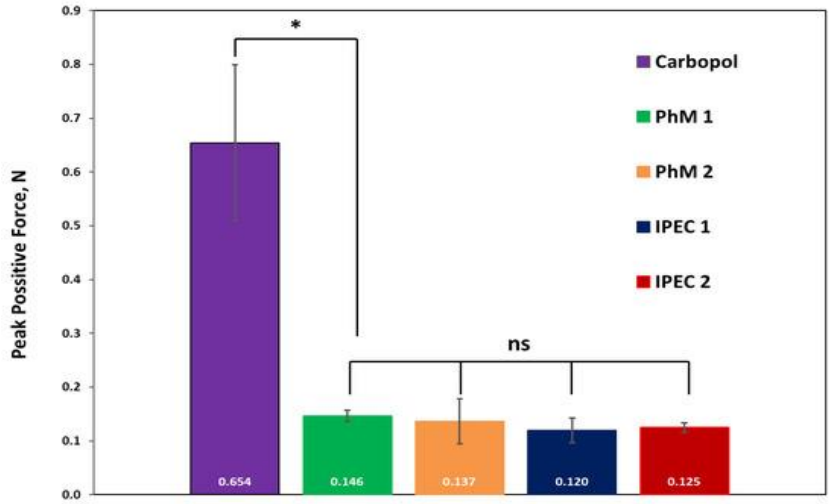

Figure 6. Results of measuring peak positive force of IPECs and PhMs from pig stomach mucosa (N) (n = 3, mean ± SD, "*" represents $P < 0.05$, "ns" represents not significant).

Study of drug release

Metronidazole (MZ) and acyclovir (ACR) both exhibit high solubility in gastrointestinal fluids. According to the Biopharmaceutics Classification System (BCS), MZ is classified as class I [48, 49], whereas ACR is classified as class III [50, 51].

The release behavior of MZ **(Figure 7)** was generally consistent across all formulations. The cumulative release reached values above 49.62% ± 6.20% for IPEC 1 matrices and 87.69% ± 5.15% for IPEC 2 matrices. In comparison, PhM-based systems released approximately 50% of the drug. These results align with previously reported behavior of highly soluble drugs such as theophylline (BCS class I) [26]. A clear relationship was observed between swelling degree and drug release rate, with higher swelling leading to faster release. The slightly irregular profile observed for IPEC 2 is likely due to partial structural breakdown of the matrix during the test.

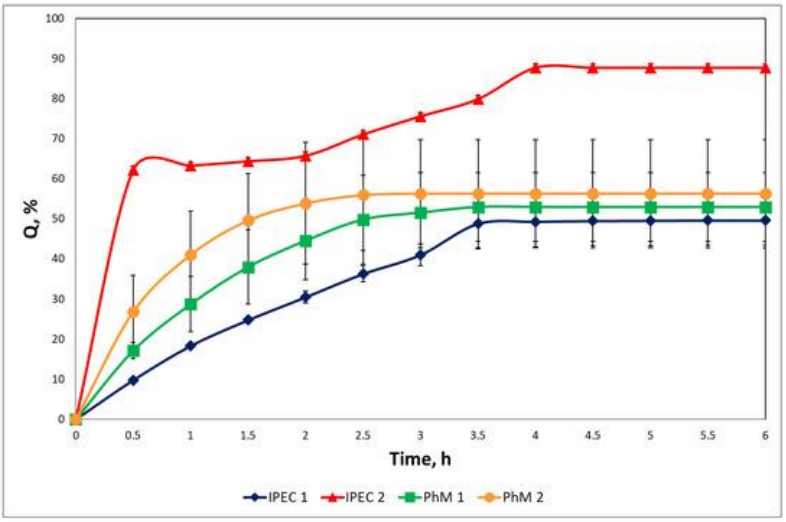

Figure 7. Release profiles of metronidazole from IPEC and PhM matrices in mimicking fasted stomach medium (0.1 M HCl) (n = 3, mean ± SD).

For acyclovir **(Figure 8)**, PhM-based matrices produced approximately 20% lower cumulative release after 6 h in acidic conditions. The total release from IPEC systems was 25.76% ± 5.67% (IPEC 1) and 21.48% ± 5.00% (IPEC 2). Although final concentrations were similar, the release kinetics differed markedly. IPEC 2 exhibited a burst-

like release during the first hour, followed by a plateau phase. In contrast, IPEC 1 showed a more controlled and continuous release over the entire 6 h period.

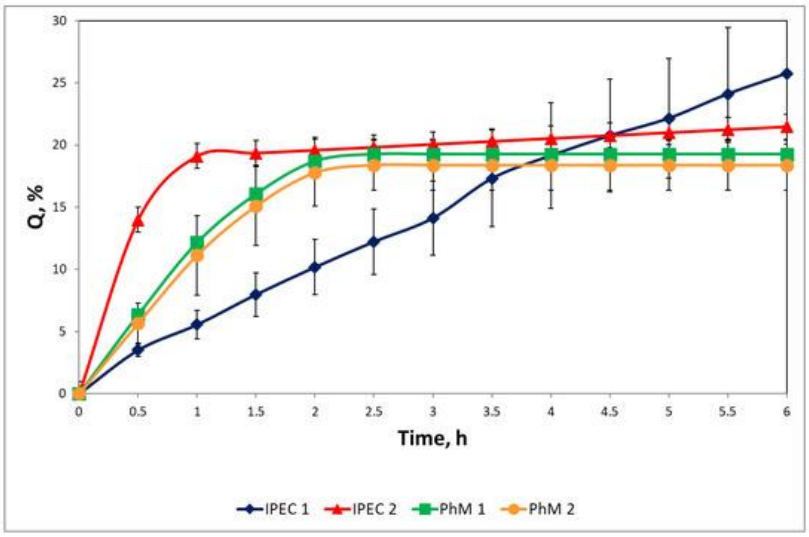

Figure 8. Release profiles of acyclovir from IPEC and PhM matrices in mimicking fasted stomach medium (0.1 M HCl) (n = 3, mean ± SD).

To clarify the release mechanism, experimental data were analyzed using zero-order, first-order, and Peppas–Sahlin kinetic models. The results of these fittings are presented in **Tables 3 and 4**.

Table 3. Results obtained from fitting experimental MZ release data.

Sample	Kinetic model	R^2
IPEC 1	Zero-order release model	0.5952
	First-order release model	0.8459
	Peppas–Sahlin model	0.9762

Table 4. Results obtained from fitting experimental ACR release data.

Sample	Model	R^2
IPEC 1	Zero-order	−17.3238
	First-order	0.9935
	Peppas–Sahlin	0.9813
IPEC 2	Zero-order	−17.3238
	First-order	−15.0387
	Peppas–Sahlin	0.9892

The modeling results showed that zero-order kinetics does not adequately describe drug release from these systems. The first-order model was only appropriate for describing ACR release from IPEC 1. Based on R^2 values, the Peppas–Sahlin model provided the best fit to release behavior for both drugs across the studied matrices.
The Peppas–Sahlin Eq. 2 describes drug release as a combination of diffusion and polymer relaxation mechanisms:

$$Q = K_1 \cdot t^m + K_2 \cdot t^{2m} \quad (2)$$

where Q is the fraction of drug released at time t, K1 and K2 are kinetic constants, and m is the diffusional exponent.
In this model, K1 represents Fickian diffusion, while K2 reflects polymer relaxation and erosion-related contributions [52].

The fitted parameters for MZ and ACR release are summarized in **Tables 5 and 6**, and the corresponding model plots are shown in **Figures 9 and 10**. Data for the MZ release from IPEC 2 are not reported because the rapid release exceeded 60% within the first hour.

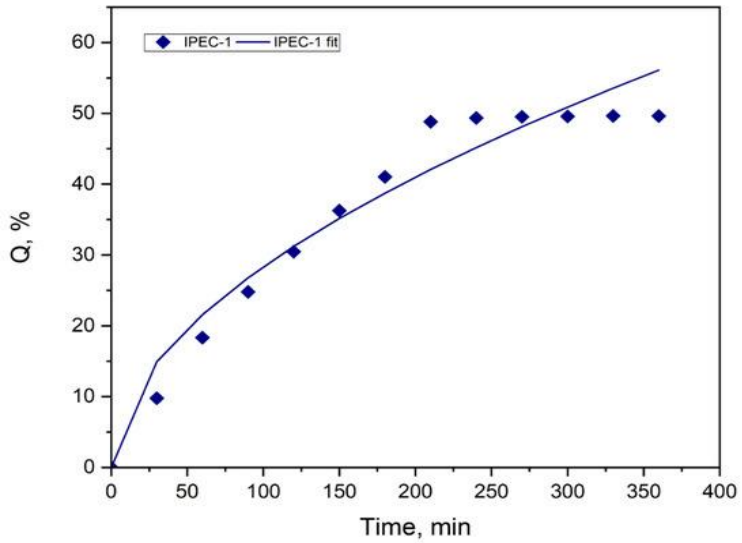

Figure 9. Release of MZ from the matrix based on IPEC 1 in mimicking fasted stomach medium (0.1 M HCl). Experimental data points and predicted data from the Peppas–Sahlin model.

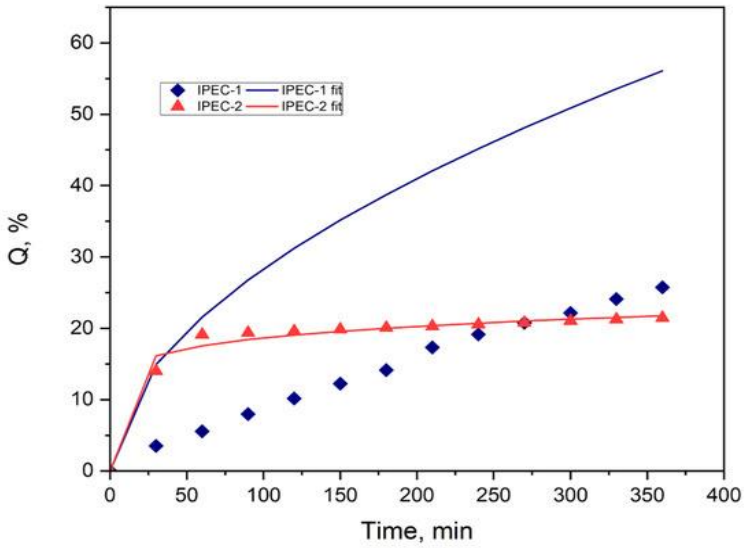

Figure 10. Release of ACR from the matrix based on IPEC 1 and IPEC 2 in mimicking fasted stomach medium (0.1 M HCl). Experimental data points and predicted data from the Peppas–Sahlin model.

Table 5. Results obtained from fitting experimental MZ release data to the Peppas–Sahlin model.

Parameters	IPEC 1
m	0.2681
K_1	0.1000
K_2	2.3675
R^2	0.9762

Table 6. Results obtained from fitting experimental ACR release data to the Peppas–Sahlin model.

Parameters	IPEC 1	IPEC 2
m	0.2681	0.0605
K_1	0.1000	0.1675
K_2	2.3676	10.5505

R^2	0.9813	0.9892

Based on R^2 values, the Peppas–Sahlin approach is suitable for describing the observed release mechanisms. The ratio between relaxation-controlled and diffusion-controlled processes (R/F) was calculated from the fitted parameters **(Figures 11 and 12)**. For both drugs and both systems, R/F values were greater than 1, indicating that polymer relaxation and erosion dominate the release mechanism. This confirms that drug liberation is mainly governed by polymer chain relaxation within the matrix. Additionally, the increasing R/F trend over time for MZ and ACR release from IPEC 1 suggests that the contribution of relaxation mechanisms becomes progressively more important during the release period [53].

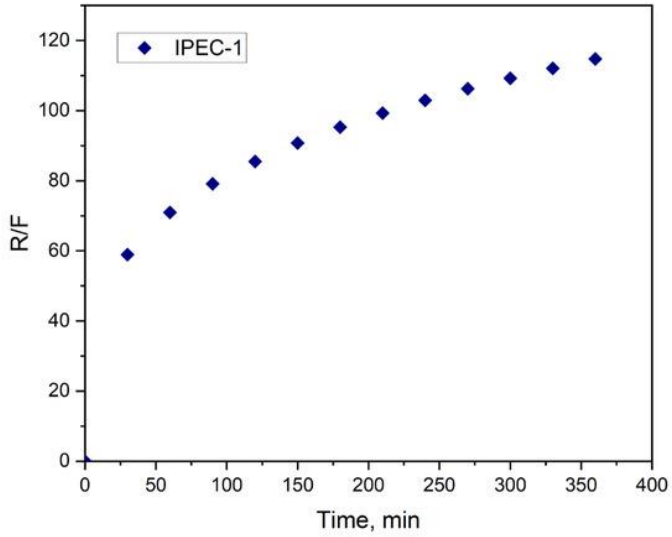

Figure 11. Relaxation contribution (R)/Fickian contribution (F) ratio over time for metronidazole release.

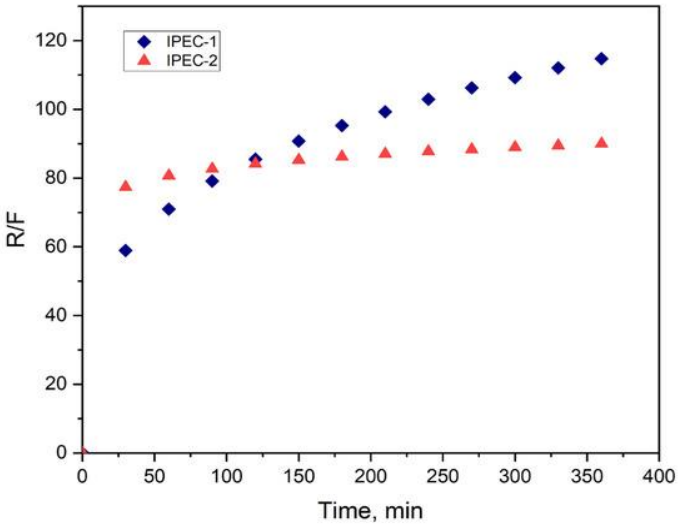

Figure 12. Relaxation (R) and Fickian (F) contributions to acyclovir release over time.

Conclusion

The obtained findings demonstrate that interpolyelectrolyte complexes based on Eudragit® EPO/L100 have clear potential as controlled-release carriers for gastroretentive drug delivery. This is supported by their appropriate swelling behavior in acidic conditions simulating the fasted stomach, as well as their adequate bioadhesive performance. Evaluation of structural and compositional changes in the polycomplexes during exposure to the tested media suggests that these materials exhibit self-healing properties. The internal structural changes observed in IPEC matrices did not act as a limiting factor and still permitted their stability in acidic environments.

The release behavior of metronidazole (MZ, class I BCS) from the IPEC matrices increased in parallel with increasing swelling degree. Among the tested systems, IPEC 1 enabled a more sustained release of MZ under simulated fasted gastric conditions (0.1 M HCl). In contrast, matrices prepared from both types of IPECs demonstrated a relatively slow release of acyclovir (ACR, class III BCS) in acidic medium, with the cumulative amount of drug released remaining below 30% over the 6 h experimental period. The release profiles of both model drugs were governed by polymer chain relaxation within the matrix, as described by the Peppas–Sahlin kinetic model. In vitro swelling and drug release studies conducted for the prepared IPEC systems further support these observations.

Overall, the investigated polycomplex systems are promising candidates for further development and assessment as carriers for gastroretentive bioadhesive drug delivery systems.

Acknowledgments: The authors are grateful to Evonik Ind. (Darmstadt, Germany) for donating samples of Eudragit® copolymers. The authors are also grateful to Alexander Sitenkov and Shamil Nasibullin for their help in the physico-chemical assessment of IPEC samples.

Conflict of Interest: None

Financial Support: The study was carried out with the financial support of the Russian Science Foundation (RSF) in the framework of research project No 23-15-00263 (D.S.G., A.V.S., and R.I.M.).

Ethics Statement: None

References

1. Alqahtani AA, Mohammed AA, Fatima F, Ahmed MM. Fused deposition modelling 3D-printed gastro-retentive floating device for propranolol HCl tablets. Polymers (Basel). 2023;15:3554.
2. Patel M, Shelke S, Shaikh F, Surti N, Panzade P, Panjwani D. Gastroretentive floating microsponges of mitiglinide: design, preparation, and pharmacokinetic evaluation. J Pharm Innov. 2023;14:1500-14.
3. Malladia M, Jukanti R. Formulation development and evaluation of a novel bi-dependent clarithromycin gastroretentive drug delivery system using Box-Behnken design. J Drug Deliv Sci Technol. 2016;35:134-45.
4. Uboldi M, Melocchi A, Moutaharrik S, Palugan L, Cerea M, Foppoli A, et al. Administration strategies and smart devices for drug release in specific sites of the upper GI tract. J Control Release. 2022;348:537-52.
5. Awasthi R, Kulkarni GT. Decades of research in drug targeting to the upper gastrointestinal tract using gastroretention technologies: where do we stand? Drug Deliv. 2016;23:378-94.
6. Naseem F, Shah SU, Rashid SA, Farid A, Almehmadi M, Alghamdi S. Metronidazole based floating bioadhesive drug delivery system for potential eradication of H. pylori: preparation and in vitro characterization. Polymers (Basel). 2022;14:519.
7. Sravya V, Suresh KP, Jagannath PV, Sunitha C. Formulate gastroretentive floating bioadhesive drug delivery system of nizatidine by direct compression technique. World J Pharm Sci. 2022;10:59-73.
8. Altreuter DH, Kirtane AR, Grant T, Kruger C, Traverso G, Bellinger AM. Changing the pill: developments toward the promise of an ultra-long-acting gastroretentive dosage form. Expert Opin Drug Deliv. 2018;15:1189-98.
9. Zhang C, Tang J, Liu D, Li X, Cheng L, Tang X. Design and evaluation of an innovative floating and bioadhesive multiparticulate drug delivery system based on hollow structure. Int J Pharm. 2016;503:41-55.
10. Patel K, Chouksey R. A recent advantage on gastroretentive drug delivery system: an overview. Res J Pharm Technol. 2023;15:36-44.
11. Pawar VK, Kansal S, Asthana S, Chourasia MK. Industrial perspective of gastroretentive drug delivery systems: physicochemical, biopharmaceutical, technological and regulatory consideration. Expert Opin Drug Deliv. 2012;9:551-65.
12. Tripathi J, Thapa P, Maharjan R, Jeong SH. Current state and future perspectives on gastroretentive drug delivery systems. Pharmaceutics. 2019;11:193.

13. Singh B, Sharma V, Mohan M, Rohit, Sharma P, Ram K. Design of ciprofloxacin impregnated dietary fiber psyllium-moringa gum-alginate network hydrogels via green approach for use in gastro-retentive drug delivery system. Bioact Carbohydr Diet Fibre. 2023;29:100345.
14. Farhaj S, Conway BR, Ghori MU. Nanofibres in drug delivery applications. Fibers. 2023;11:21.
15. Das S, Kaur S, Rai VK. Gastro-retentive drug delivery systems: a recent update on clinical pertinence and drug delivery. Drug Deliv Transl Res. 2021;11:1849-77.
16. Pal R, Pandey P, Nogai L, Arushi, Anand A, Suthar P, et al. The future perspectives and novel approach on gastro retentive drug delivery system (GRDDS) with current state. Can J Clin Pharmacol. 2023;30:594-613.
17. Zhu X, Qi X, Wu Z, Zhang Z, Xing J, Li X. Preparation of multiple-unit floating-bioadhesive cooperative minitablets for improving the oral bioavailability of famotidine in rats. Drug Deliv. 2014;21:459-66.
18. Darbasizadeh B, Motasadizadeh H, Foroughi-Nia B, Farhadnejad H. Tripolyphosphate-crosslinked chitosan/poly(ethylene oxide) electrospun nanofibrous mats as a floating gastro-retentive delivery system for ranitidine hydrochloride. J Pharm Biomed Anal. 2018;153:63-75.
19. Meng S, Wang S, Piao MG. Prescription optimization of gastroretentive furosemide hollow-bioadhesive microspheres via Box-Behnken design: in vitro characterization and in vivo evaluation. J Drug Deliv Sci Technol. 2022;70:103235.
20. Ngwuluka NC, Choonara YE, Modi G, du Toit LC, Kumar P, Ndesendo VMK, et al. Design of an interpolyelectrolyte gastroretentive matrix for the site-specific zero-order delivery of levodopa in Parkinson's disease. AAPS PharmSciTech. 2013;14:605-19.
21. Gallardo D, Skalsky B, Kleinebudde P. Controlled release solid dosage forms using combinations of (meth)acrylate copolymer. Pharm Dev Technol. 2008;13:413-23.
22. Siepmann F, Siepmann J, Walther M, MacRae RJ, Bodmeier R. Polymer blends for controlled release coatings. J Control Release. 2008;125:1-15.
23. Mustafin RI. Interpolymer combinations of chemically complementary grades of Eudragit copolymers: a new direction in the design of peroral solid dosage forms of drug delivery systems with controlled release. Pharm Chem J. 2011;45:285-95.
24. Moustafine RI. Role of macromolecular interactions of pharmaceutically acceptable polymers in functioning oral drug delivery systems. Russ J Gen Chem. 2014;84:364-7.
25. Moustafine RI, Kabanova TV, Kemenova VA, Van den Mooter G. Characteristics of interpolyelectrolyte complexes of Eudragit E100 with Eudragit L100. J Control Release. 2005;103:191-8.
26. Moustafine RI, Bukhovets AV, Sitenkov AY, Kemenova VA, Rombaut P, Van den Mooter G. Eudragit E PO as a complementary material for designing oral drug delivery systems with controlled release properties: comparative evaluation of new interpolyelectrolyte complexes with countercharged Eudragit L100 copolymers. Mol Pharm. 2013;10:2630-41.
27. Sauer D, McGinity JW. Properties of theophylline tablets dry powder coated with Eudragit E PO and Eudragit L100-55. Pharm Dev Technol. 2009;16:632-41.
28. Obeidat WM, Abu Znait AH, Sallam AA. Novel combination of anionic and cationic polymethacrylate polymers for sustained release tablet preparation. Drug Dev Ind Pharm. 2008;34:650-60.
29. Obeidat WM, Abu Znait AH, Sallam AA. Sustained release tablets containing soluble polymethacrylates: comparison with tableted polymethacrylate IPEC polymers. AAPS PharmSciTech. 2010;11:54-63.
30. Bani-Jaber AH, Alkawareek MJ, Al-Gousous JJ, Abu Helwa AY. Floating and sustained-release characteristics of effervescent tablets prepared with a mixed matrix of Eudragit L100-55 and Eudragit E PO. Chem Pharm Bull (Tokyo). 2011;59:155-60.
31. Bani-Jaber AH, Al-Aani L, Alkhatib H, Al-Khalidi B. Prolonged intragastric drug delivery mediated by Eudragit E carrageenan polyelectrolyte matrix tablets. AAPS PharmSciTech. 2011;12:354-61.
32. Quinteros DA, Manzo RH, Allemandi DA. Interaction between Eudragit E100 and anionic drugs: addition of anionic polyelectrolytes and their influence on drug release performance. J Pharm Sci. 2011;100:4664-73.
33. Wulff R, Leopold CS. Coatings from blends of Eudragit RL and L55: a novel approach in pH-controlled drug release. Int J Pharm. 2014;476:78-87.
34. Wulff R, Leopold CS. Coatings of Eudragit RL and L55 blends: investigations on the drug release mechanism. AAPS PharmSciTech. 2016;17:493-503.

35. García MC, Martinelli M, Ponce NE, Sanmarco LM, Aoki MP, Manzo RH, et al. Multi-kinetic release of benznidazole-loaded multiparticulate drug delivery systems based on polymethacrylate interpolyelectrolyte complexes. Eur J Pharm Sci. 2018;120:107-22.
36. Sester C, Ofridam F, Lebaz N, Gagnière E, Mangin D, Elaissari A. pH-sensitive methacrylic acid-methyl methacrylate copolymer Eudragit L100 and dimethylaminoethyl methacrylate, butyl methacrylate, and methyl methacrylate tri-copolymer Eudragit E100. Polym Adv Technol. 2020;31:440-50.
37. Bukhovets AV, Fotaki N, Khutoryanskiy VV, Moustafine RI. Interpolymer complexes of Eudragit copolymers as novel carriers for colon-specific drug delivery. Polymers (Basel). 2020;12:1459.
38. Gordeeva DS, Sitenkova AV, Moustafine RI. Interpolyelectrolyte complexes based on Eudragit copolymers as carriers for bioadhesive gastroretentive metronidazole delivery system. Drug Dev Regist. 2020;9:72-6.
39. Lankalapalli S, Kolapalli VRM. Polyelectrolyte complexes: a review of their applicability in drug delivery technology. Indian J Pharm Sci. 2009;71:481-7.
40. De Robertis S, Bonferoni MC, Elviri L, Sandri G, Caramella C, Bettini R. Advances in oral controlled drug delivery: the role of drug-polymer and interpolymer non-covalent interactions. Expert Opin Drug Deliv. 2015;12:441-53.
41. Porfiryeva NN, Nasibullin SF, Abdullina SG, Tukhbatullina IK, Moustafine RI, Khutoryanskiy VV. Acrylated Eudragit E PO as a novel polymeric excipient with enhanced mucoadhesive properties for application in nasal drug delivery. Int J Pharm. 2019;562:241-8.
42. Porfiryeva NN, Semina II, Salakhov IA, Moustafine RI, Khutoryanskiy VV. Mucoadhesive and mucus-penetrating interpolyelectrolyte complexes for nose-to-brain drug delivery. Nanomedicine. 2021;37:102432.
43. Shin S, Kim TH, Jeong SW, Chung SE, Lee DY, Kim DH, et al. Development of a gastroretentive delivery system for acyclovir by 3D printing technology and its in vivo pharmacokinetic evaluation in Beagle dogs. PLoS One. 2019;14:e0216875.
44. Farshforoush P, Ghanbarzadeh S, Goganian AM, Hamishehkar H. Novel metronidazole-loaded hydrogel as a gastroretentive drug delivery system. Iran Polym J. 2017;26:895-901.
45. Peppas NA, Sahlin JJ. A simple equation for the description of solute release. III. Coupling of diffusion and relaxation. Int J Pharm. 1989;57:169-72.
46. Zhang Y, Huo M, Zhou J, Zhou A, Li W, Yao C, et al. DDSolver: an add-in program for modeling and comparison of drug dissolution profiles. AAPS J. 2010;12:263-71.
47. Boddupalli BM, Mohammed ZN, Nath RA, Banji D. Mucoadhesive drug delivery system: an overview. J Adv Pharm Technol Res. 2010;1:381-7.
48. Zhang S, Fang M, Zhang Q, Li X, Zhang T. Evaluating the bioequivalence of metronidazole tablets and analyzing the effect of in vitro dissolution on in vivo absorption based on PBPK modeling. Drug Dev Ind Pharm. 2019;45:1646-53.
49. Sulistiawati, Dwipayanti KS, Azhar M, Rahman L, Pakki E, Himawan A, et al. Enhanced skin localization of metronidazole using solid lipid microparticles incorporated into polymeric hydrogels for potential improved rosacea treatment: an ex vivo proof of concept investigation. Int J Pharm. 2022;628:122327.
50. Wu F, Cristofoletti R, Zhao L, Rostami-Hodjegan A. Scientific considerations to move towards biowaiver for biopharmaceutical classification system class III drugs: how modeling and simulation can help. Biopharm Drug Dispos. 2021;42:118-27.
51. Mady OI, Osman MA, Sarhan NI, Shatla AA, Haggag YA. Bioavailability enhancement of acyclovir by honey: analytical and histological evidence. J Drug Deliv Sci Technol. 2023;80:104155.
52. Filippova NI, Teslev AA. Application of mathematical modeling in the evaluation of in vitro drug release. Drug Dev Regist. 2017;4:218-26.
53. Unagolla JM, Jayasuriya AC. Drug transport mechanisms and in vitro release kinetics of vancomycin encapsulated chitosan-alginate polyelectrolyte microparticles as a controlled drug delivery system. Eur J Pharm Sci. 2018;114:199-209.